

Carrier Effect on Structure and Properties of Heat-Treated Poly(Ethylene Terephthalate) Fibers. I. Thermal Analysis and Dynamic Mechanical Properties

MÁRCIA SILVA DE ARAÚJO* and ABIGAIL LISBÃO SIMAL†

Universidade Federal de São Carlos, DEMa, cx.postal 676, 13560-905, São Carlos, Sp., Brazil

SYNOPSIS

Poly(ethylene terephthalate) (PET) fibers of different draw ratios (as spun and drawn 2.8×) were submitted to different heat settings. Subsequently, they were treated in benzoic acid solutions at different concentrations and for different times of exposition. The plasticizing effect on the morphology of these heat-set fibers due to the different treatments in benzoic acid solutions was studied by differential scanning calorimetry (DSC) and dynamic and mechanical thermal analysis (DMTA). The DSC experiments revealed the appearance of a premelting peak (pm1) around 130°C, when the applied heat settings were carried out for 8 h in the presence of boiling water, and around 150–160°C for the dry heat setting for 7 h at 130°C followed by 1 h in the presence of boiling water. These premelting peaks have been associated with the melting of smaller and imperfect crystals present in the amorphous region. Also, the analysis of the main melting peaks revealed that the undrawn fiber presented a wider distribution of smaller crystals than the drawn one. Their subsequent treatments in the benzoic acid solutions revealed through the DSC thermograms that this first premelting peak tends to disappear as the concentration and time of benzoic acid treatment increase. Also, a new premelting peak (pm2) appears in the DSC thermograms at temperature around 180°C. It seems that a dislocation of the pm1 peak is occurring toward higher temperatures and is being transformed in this new premelting peak. The DMTA revealed the appearance of an α_c transition in the temperature range from 140 to 160°C and this α_c transition seems to be related to the relaxations of the new crystallites formed due to the plasticization effect of the benzoic acid. Also, the second premelting peak seems to be related to the fusion of such crystals. Therefore, a complex change in the morphology of the studied PET fibers due to the benzoic acid action has been revealed. © 1996 John Wiley & Sons, Inc.

INTRODUCTION

Carriers have been used frequently in the textile industry in order to accelerate the dyeing process, especially polyesters and acrylics, which are more difficult to dye because of their low rates of dye sorption at normal dyeing temperatures. Carriers are low-molecular-weight compounds that work as a plasticizer, reducing the glass transition of the fiber and

increasing chain flexibility; consequently, acceleration of the dye diffusion will be achieved. Benzoic acid belongs to the class of water-soluble carriers, which requires it to be used in large concentrations.¹ The use of such compounds at high concentrations and for long times at dyeing temperatures (100°C) can induce structural changes, such as increase of crystallinity of the poly(ethylene terephthalate) (PET) fibers.² These structural changes can affect the dyeing process by decreasing the diffusion coefficient. Therefore, the knowledge of the structural changes due to benzoic acid action is of great interest.

Some studies^{3–7} on PET fibers have shown the appearance of a premelting peak on differential

* Present address: DEMa/Univ. Estadual de Ponta Grossa, PR, Brazil.

† To whom correspondence should be addressed.

scanning calorimetry (DSC) analysis prior to the main melting peak when these fibers are submitted to different heat treatments, in the presence or absence of a plasticizer. Weigmann et al.³ have shown that depending on the nature of the treatment and temperature, crystallites are formed in PET fibers varying in size and thermal stability. If there are enough of such crystallites, they can be observed in the DSC thermogram in the form of a small pre-melting peak at a temperature significantly below the actual melting peak. Their PET fibers were treated in the presence of dimethyl formamide (DMF) followed by heat treatments in silicone oil at different temperatures. So, the DMF treatments produced, in addition to voids, the formation of crystallites with a wide distribution of sizes, which would appear as a pre-melting peak in a DSC thermogram. The subsequent heat treatments cause a partial collapse of voids.

In a subsequent work, Weigmann et al.⁴ submitted their PET fibers to a DMF treatment after heat setting in the presence of silicone oil. In this particular case, the pre-melting peaks produced by the heat treatments at temperatures below 180°C were eliminated by the subsequent DMF treatment, suggesting that crystallites of low stability produced during the heat treatments were melting out by the solvent treatment. The stabilization of these crystallites to a subsequent DMF treatment would occur only when the applied heat treatments were realized at higher temperatures. Although the DMF is a strong interacting plasticizer,^{3,4} contrary to the benzoic acid¹ utilized in this work, it is possible to expect some similarities in their influence on the structure of the PET fibers.

Oswald et al.⁵ have concluded in their work that the appearance of the pre-melting peak might be related to the melting of very small crystallites (nuclei-sized crystallites) which would be located in the highly strained amorphous domains, which persist after heat treatments. Also, Rao et al.⁶ have pointed out a wide range of views concerning the nature and origin of these pre-melting endothermic transitions, presenting yet their own view on the subject. They have related the pre-melting endotherm for their heat-setted PET fibers to the melting of smaller or imperfect crystals in favor of the formation of larger and more perfect crystals. Gacén et al.⁷ have associated the temperatures where the pre-melting occurs to the ultimate temperature where the fibers can present thermal stability.

Although there are some differences in the presented theories, there appears to be a consensus that the observed pre-melting peak is representative of

the melting of small crystallites which would be formed by the different applied heat treatments. These theories concerning the appearance of such pre-melting peaks will be very helpful to promote a better understanding of the benzoic acid action on the morphology of our PET fibers.

So, in the present work, the PET fibers with different draw ratios were submitted initially to different preheat settings in order to avoid structural changes due to boiling water action. Subsequently they were exposed to different concentrations of benzoic acid solution at different times, their structural changes due to benzoic acid action were studied through DSC and dynamic and mechanical thermal analysis (DMTA), and the results are presented.

EXPERIMENTAL

Sample Preparation

PET fibers from Rhodia S/A. (Sto. André/SP-Brazil) of different draw ratios (as spun, and 2.8×) and title of 75 dtex were submitted to different heat treatments under slack conditions for 8 h. A wet heat treatment (T1) was carried out in presence of distilled water at boiling temperature (98°C) for 8 h. Also, for analysis and comparison of the results, a dry heat treatment for 7 h (T2) in an evacuated oven under inert atmosphere at $130 \pm 2^\circ\text{C}$ was considered. These samples, after treatment T2 had been submitted to an additional 1-h treatment in boiling water (T3), totaled the same 8 h utilized in T1.

The choice of the heat treatment times was based on previous works on PET fibers^{2,8} where the fibers were considered structurally stable after 6 h of dry treatment. Knox and colleagues⁹ have demonstrated also that the PET fibers wet treated in the boiling water temperature for times above 10 h can show accentuated hydrolysis of ester groups, which would decrease the molecular weight. Thus, the choice of time (8 h) utilized in this work for the heat settings seems to be in a safe range in order to achieve structural stability and to avoid accentuated loss of molecular weight as described by Knox et al.⁹

The achievement of a prior structural stability was necessary in order to consider in the analysis the structural changes due to the benzoic acid action only (carrier). Therefore, the heat-setted fibers (from treatments T1 and T3) were submitted to subsequent treatments in benzoic acid at different concentrations (5, 10, and 20 g/L for the as-spun fiber and 10, 20, and 30 g/L for the 2.8× drawn fiber) and times (0, 5, 24, and 48 h).

Structural Measurements

Shrinkage and Swelling

Shrinkage and swelling measurements were made by knowing the length and the diameter of the fibers before and after the heat treatments.

Therefore the shrinkage ($\%S_h$) and swelling ($\%S_w$) percentages were calculated through the following expressions:

$$\%S_h = \frac{S_h^o - S_h^f}{S_h^o} \times 100 \quad (1)$$

$$\%S_w = \frac{S_w^o - S_w^f}{S_w^o} \times 100 \quad (2)$$

where S_h^o and S_w^o = initial length and diameter of the fiber, and S_h^f and S_w^f = final length and diameter of the fiber. Polarized light microscopy was used in the diameter calculations.

DSC

DSC (from Perkin-Elmer) measurements were used to obtain the thermograms and to calculate the crystallinities from the observed areas under the heat of fusion peaks (ΔH_f) of the samples. The crystallinity percentages ($\%C$) were calculated as follows:

$$\%C = \frac{\Delta H_f}{\Delta H_o} \times 100 \quad (3)$$

where ΔH_o = value of the heat of fusion for the total crystalline PET or 28.1 kcal/mol.¹⁰

ΔH_f = the observed heat of fusion in kcal/mol. The runnings were effectuated under inert atmosphere at a heating rate of 10°C/min.

DMTA

DMTA (from Polymer Laboratories) runnings were used to evaluate the dynamic and mechanical properties of the samples through E' , E'' , and $\tan \delta$ measurements. The conditions of the runnings were heating rate of 3°C/min and frequency of 10 Hz.

X-Ray Analysis

X-ray diffraction method was performed with Carl Zeiss Jena equipment, utilizing an Ni-filtered Cu $K\alpha$ radiation. The results were analyzed by the diffractometric method.

Wide-angle x-ray scattering measurements were used to calculate the crystallinity index (CI), crystal size (CS), and lateral order (LO) as de-

scribed in detail in the literature.¹¹⁻¹⁴ Our PET fibers presented a characteristic three-peak equatorial x-ray scattering pattern as described by Cullerton et al.¹¹ and Bhat and Naik.¹⁴ The observed peak maxima were: $2\theta_1 \cong 17.5^\circ$, $2\theta_2 \cong 22.5^\circ$, and $2\theta_3 \cong 25.5^\circ$ which correspond to the crystal planes (010), (110), and (100), respectively.¹⁴ Although, much more precise methods for crystallinity determinations can be found in the literature,¹² the method utilized by Cullerton and colleagues¹¹ was chosen due its simplicity. This method assumes a two-phase model for the fiber and involves separating the scattering diagram into relative crystalline and amorphous components. The width of the crystalline peak at $2\theta \cong 17.5^\circ$ was considered for the CS calculations, through the basic Scherrer equation¹² or:

$$CS = \frac{K\lambda}{\beta \cos \theta} \quad (4)$$

where K is a shape factor which varies between 0.9 and 1.1. A value of 1.0 has been considered for our calculations. λ = wavelength of the radiation used (Cu $K\alpha$ = 1.5418 Å), β = half-maximum breadth in radians, and θ = Bragg's angle.

The crystalline size measurement corresponds to the direction perpendicular to the plane (010) chosen for the calculations. The calculated values of the CS should be considered as relative values only, since the necessary corrections for the Scherrer equation¹² were not made.

The LO^{13,14} parameter can be related to several factors at the same time, such as the crystallinity of the samples, perfection, size, and distribution of the crystallites, and it was calculated from the following equation:

$$\%LO = (1 - RF) \times 100 \quad (5)$$

where RF is the resolution factor which is given by the following expression:

$$RF = \frac{m_1 + 2m_2 + m_3 + \dots + m_n - 1}{h_1 + h_2 + h_3 + \dots + h_n} \quad (6)$$

where m_1 , m_2 , etc., are the heights of minima from the appropriate baseline, and h_1 , h_2 , etc., are the heights of maxima from the same baseline. Therefore, this resolution factor for our PET fibers can be written as follows:

$$RF = \frac{m_1 + 2m_2}{h_1 + h_2 + h_3} \quad (7)$$

where m_1 and m_2 correspond to the minima between the planes (010) and (110) and between the planes (110) and (100), respectively. The variables h_1 , h_2 , and h_3 are the observed maxima diffraction peaks correspondent to be planes (010), (110), and (100).

When the resolution is absent, RF tends to be 1, and RF tends to be zero when the resolution is maximum. Thus, RF is inversely related to the LO^{13} . Some authors^{13,14} have used this parameter as a substitution for the crystalline index measurement. In this case, it is being considered the total order rather than the absolute crystallinity. In our study, it was considered both parameters.

Fourier Transform Infrared

Fourier transform infrared (FTIR) from Bomem-Michelson 102 equipped with a polarizer from Perkin Elmer was used to evaluate the ratio between the trans and gauche content in the PET fibers. The trans conformation can be present in both regions, amorphous and crystalline, and is related to the straight parts of the molecule. The gauche conformation can be present in the amorphous region only and is related to the bended or distorted parts of the molecule.¹⁵ The changes in the absorption ratio between the trans and gauche conformers can be used to quantify the conformational changes during the crystallization process due to heat treatments. The bands near 1473, 1343, 973, and 848 cm^{-1} have been referred to in the literature¹⁵ as vibrational modes of the trans ethylene glycol segment of the polymer chain, and the bands near 1453, 1372, 1042, and 898 cm^{-1} refer to the vibrations of the gauche ethylene glycol segment of the polymer chain.¹⁶ For this study, the bands 973 cm^{-1} and 898 cm^{-1} were chosen to calculate the structural absorbances (A_o) of the trans and gauche conformations, respectively, in accordance with the following expression¹⁷:

$$A_o = \frac{A_{//} + 2A_{\perp}}{3} \quad (8)$$

The structural absorbance was determined in order to remove the effects of orientation concerning the spectra of the samples with cylindrical symmetry.¹⁷ All of the calculated structural absorbances can be corrected by an internal reference,¹⁷ which is necessary to compensate for the sample thickness. This correction is particularly important for quantitative calculations of the content of a particular band (trans or gauche conformers) and the calculation of the dichroic function (DF), as expressed by the following equation:

$$DF = \frac{R - 1}{R + 2} \quad (9)$$

where R is the dichroic ratio defined as the quotient of the extinction values of an absorption band for the parallel ($A_{//}$) and perpendicular (A_{\perp}) vibration directions of the infrared spectrum.

The DF has been mentioned in the literature¹⁷⁻¹⁹ to represent orientation data, because of its proportionality to the orientation function.¹⁷ This approach is particularly useful in the case of uncertainty about the exact transition band, which is necessary for the calculation of the orientation function¹⁷ as expressed by the following equation:

$$f = \left(\frac{R - 1}{R + 2} \right) / \left(\frac{R_o - 1}{R_o + 2} \right) \quad (10)$$

where $R_o = 2 \cot^2 \alpha$ represents the dichroic ratio of the absorption band ideally oriented, and α is the angle between the transition moment and the molecular axis. Therefore, eq. (10) can be reduced to eq. (9), when the analyzed band is a π type, where $R_o = \infty$ and $\alpha < 54.7^\circ$.^{19,20}

In this study, eq. (9) was applied to estimate the orientation of the amorphous region of our PET fibers through the 898 cm^{-1} band, which is a π -type band and representative of the gauche conformation.

The internal reference band utilized for the calculations was the 1506 cm^{-1} ¹⁸ band, with π polarization and designated to the vibrational mode of the benzenic ring.²⁰ The reference band chosen should be a band independent of changes in physical structure, such as those representing trans, gauche, and folded conformations. Therefore, the most suitable specie is the benzene part of the molecule.²⁰

RESULTS AND DISCUSSION

Morphology of the Heat-Setted Fibers

The Structural Changes Due to the Heat Treatments

Table I shows the structural changes of the fibers due to the different heat settings. The results presented in Table I will help us to understand later the structural changes of the previously heat-setted fibers (as spun, 2.8 \times) due to benzoic acid action. As expected the structural changes due to the preheat settings were higher in the as-spun fiber (0 \times). The heat treatments T1 and T2 (wet and dry, respectively) promoted shrinkage in the fibers during the

Table I Structural Changes of the PET Fibers After the Heat Treatments: T1, T2, and T3^a

Fibers	Heat Treatment	S_h (%)	S_w (%)	CI (%)	T_g (°C)	CS (Å)	LO (%)	DFa	$\frac{A_0(973)}{A_0(898)}$ (%)
0x	Control	—	—	0	86	—	—	0.03	19.0
	T ₁	61.5	50	47	102	30	20	0.20	41.0
	T ₂	60.3	48	48	103	35	25	-0.02	37.7
	T ₃	60.4	53	47	98	32	26	0.05	49.7
2.8x	Control	—	—	34	104	37	5	0.11	45.6
	T ₁	10.8	12	57	129	34	23	0.46	50.5
	T ₂	12.8	10	63	128	41	24	0.26	76.2
	T ₃	15.2	12	63	128	41	30	0.19	60.3

^a % S_h , shrinkage percentage; % S_w , swelling percentage; $\frac{A_0(973)}{A_0(898)}$, structural absorbance ratio of the 973 cm⁻¹/898 cm⁻¹ (trans/gauche) absorption bands (in percentage).

crystallization process. However, the undrawn (0×) fiber showed higher shrinkage values (about five to six times) than the drawn one. This behavior is a result of the structural instability of the 0× fiber, due to the lack of drawing. The different heat treatments (wet and dry) seem to promote the same level of structural changes in both fibers.

The observed changes in the percentage of structural absorbance ratio between the trans and gauche absorption bands reflect the conformational changes during the crystallization process due to the applied heat treatments. The structural absorption ratio data show an accentuated increase of the trans conformation for the different heat treatments applied to the samples. Based on the convenient two-phase model for semicrystalline yarns,¹⁵ the trans conformation can be present in both regions, amorphous and crystalline, and is related to the straight parts of the molecules, while the gauche conformation reflects the disorganized parts of the molecules present in the amorphous region only. Therefore, it seems that the chains located in the amorphous regions are being pulled from their original and more random conformation to a new and more oriented one, probably in the orientation direction of the crystalline phase being developed due to the applied heat settings. Also, it is possible to observe from these data on structural absorbance ratios that the dry heat treatment (T2) is more effective in the increasing of the trans conformer content for the 2.8× fiber than the as-spun one.

Lin and Koenig¹⁶ have demonstrated that the trans isomer allows a closer packing of the polymer chains than the gauche isomer. So, the trans isomers are more affected by the changes in the intermolecular distance than are the gauche isomers. The dry

treatment applied to the drawn sample seems to be more effective in increasing intermolecular packing by decreasing intermolecular distance, and the presence of a previous orientation in the fiber favors such closer packing. Since the trans conformation can be present in both regions, amorphous and crystalline, the increase in the structural absorbance ratio for the drawn sample might be associated with the overall packing.

When the originally drawn fiber is submitted to the heat treatment T3 (dry treatment T2, followed by a boiling water treatment), a decrease in the trans conformer is observed. Therefore, the water treatment might be affecting the chain packing of the amorphous region of this fiber, since it can be expected that the water molecules will permeate more easily through their amorphous regions. The swelling data seem to be in accordance with this behavior. Also, the observed decrease in the amorphous DF for this heat treatment reinforces such a conclusion.

Another interesting observation from the data presented on Table I is that the heat treatments T2 and T3 seem to be affecting differently the as-spun fiber, concerning the amount of trans conformer. For this fiber, the subsequent 1 h treatment in boiling water (treatment T3) is causing an increase of trans conformation, contrary to the observed behavior of the drawn fiber as discussed above. Therefore, one could suspect that the differences in orientation are the commanding factor in such behavior. However, it is not possible to confirm with certainty where this increase in the amount of trans conformer is occurring more effectively, in the amorphous or in the crystalline regions.

Since there was a 5% increase in swelling when this dry heat-treated fiber was submitted to a sub-

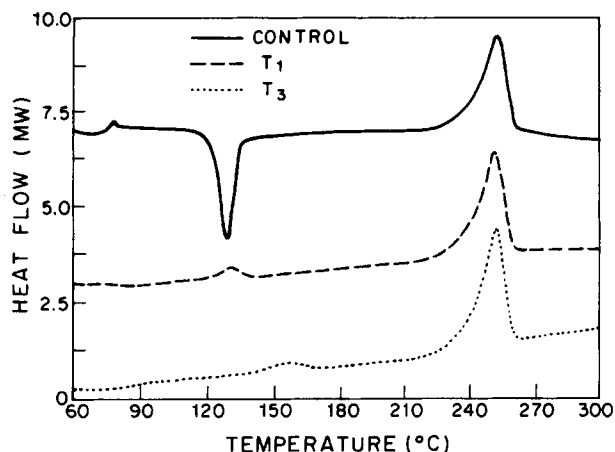


Figure 1 DSC thermograms of the as-spun fiber control and after applied heat treatments (T1 and T3).

sequent 1 h boiling water treatment, it is possible to draw the hypothesis that the increase of trans conformer might be occurring preferentially in the crystalline region. The swelling might be an indication of void formation, with a consequent bending and loosening of the chains in the amorphous region, which would not favor an increase of trans conformation in this region. Also, the insignificant changes observed for the Dfa parameter when this fiber is submitted to treatment T3 seem to be in accordance with such a hypothesis.

As can be observed from Table I, the values of the CS, LO, and CI remain practically at the same levels for treatments T2 and T3. Thus, this fact might be an indication that the observed increase in the trans conformation in the crystalline region due to the additional 1 h boiling water treatment (T3) can be related to an increase of perfection of crystals. The absence of orientation and the less stable structure of the as-spun fiber favors such behavior, i.e., the morphological transformations occurring in the crystalline region due to the plasticization effect of the boiling water will be more easily reached.

The heat treatments also promoted an increase of glass transition temperature (T_g) as a consequence of the crystallinity increase. The small decrease of T_g observed for the as-spun fiber after treatment T3 might be related to the events occurring in the amorphous region as previously discussed, as well as to the type of crystalline structure being formed.

The DSC results presented below will help us to better understand this crystalline structure developed after the applied heat settings in both fibers.

The DSC Analysis of the Heat-Treated PET Fibers

Figures 1 and 2 show the DSC thermograms for both fibers. The thermograms show the formation of a premelting peak (pm1) in the temperature range around 130°C for the fibers treated for 8 h in boiling water (T1) and around 150–160°C for treatment T3. They are occurring at temperatures about 30°C above the temperatures of the applied heat treatments and are much more intense and well defined for the undrawn fiber. Such premelting peaks have been already described by other authors³⁻⁷ for heat-treated polyester fibers.

Some theories³⁻⁷ have already been proposed for the appearance of such premelting peaks. All of the presented theories agree that the premelting peaks can be associated with the melting of smaller and imperfect crystals and that these very small crystals (or crystallites) might be located in the amorphous regions still present after the heat treatments.⁵ The temperature range where it is occurring could correspond to the ultimate temperature where the fibers can present thermal stability, as described by Gácen and coworkers.⁷ Also, the absence of orientation might be favoring the formation of larger amounts of such small crystallites in the as-spun fiber, as revealed by its more intense premelting peak.

As can be seen in Figures 1 and 2, the temperatures of the main melting peaks remain constant for all of the applied heat settings, for the fibers with the same draw ratios. Also, the figures show that the heat of fusions of the fibers (area under the peaks) is dependent on the crystallinities and the distribution of the CS. A large range of melting temperature has been associated with a wide distribution of small crystals and a small range has been asso-

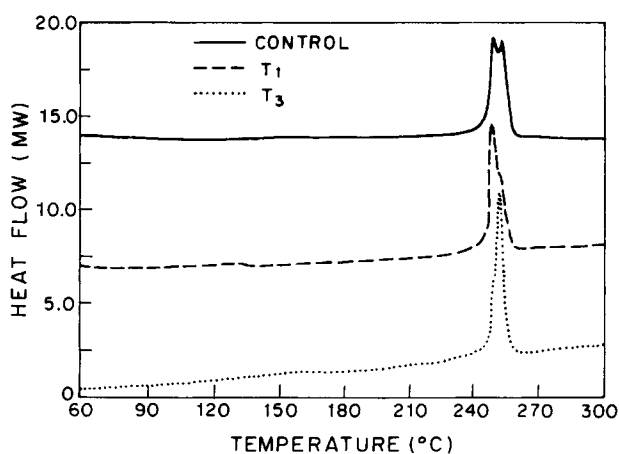


Figure 2 DSC thermograms of the 2.8 \times fiber control and after applied heat treatments (T1 and T3).

Table II Values as a Function of the Concentration and Time of Exposition in Benzoic Acid at Boiling Water Temperature^a

Fibers Preheat Treatment		0x		2.8x	
C ^b (g/L)	t ^c (h)	T1 <i>T_g</i> (°C)	T3 <i>T_g</i> (°C)	T1 <i>T_g</i> (°C)	T3 <i>T_g</i> (°C)
0	0.0	102	98	129	128
5	0.5	92	88		
	24.0	94	92	—	—
10	0.5	77	79	123	118
	24.0	79	79	116	116
	48.0	—	—	115	115
20	0.5	61	65	102	103
	24.0	—	—	87	94
	48.0	—	—	87	87
30	0.5	—	—	83	87
	24.0	—	—	75	73
	48.0	—	—	77	77

^a *T_g*, measured at temperature where *E''* is maximum by DMTA.

^b C, benzoic acid concentration in g/L.

^c t, time of treatment in benzoic acid in hours.

ciated with a narrow distribution of larger crystals.⁶ Following such a proposed theory, it is possible to affirm that the undrawn fiber presented a wider distribution of smaller crystals than the 2.8× fiber. Table I confirms, through the x-ray results, the smaller CS of the as-spun fiber.

Therefore, the applied heat treatments seem to be generating a new structure for both fibers. Very small and imperfect crystallites are being formed in addition to the bigger crystallites, which are responsible for the main melting peak, and these effects are occurring much more easily in the as-spun fiber.

The Carrier Action: Time and Concentration Effects

The DMTA

Table II shows the changes in the *T_g* values measured by DMTA (temperature where *E''* is maximum) as a function of the time and concentration of benzoic acid.

The analyzed fibers (controls) were those that underwent the preheat treatments T1 and T3, as described in the first part of this work, i.e., the fibers that were structurally stabilized in boiling water. In pretreatment T1, as already described, the fibers

were exposed for 8 h in a flask containing boiling water, and in pretreatment T3, the fibers were dry treated in an evacuated oven at 130°C for 7 h under inert atmosphere plus 1 h of exposition in boiling water.

The results of Table II show that the plasticization effect of the benzoic acid in the preheat-settled as-spun fiber (decrease of *T_g*) occurs in the first half hour of exposition in the benzoic acid solution, for all analyzed concentrations and different preheat treatments (T1 and T3) applied. A small increase of *T_g* is observed for these fibers after 24 h of treatment in the different concentrations of benzoic acid. Also, Table II reveals that the plasticization effect of the benzoic acid in the drawn fibers (2.8×) occurs for longer times of exposition in this carrier, i.e., the *T_g* decreases continuously after up to 24 h of treatment in benzoic acid solution for all concentrations and preheat settings studied (T1 and T3).

Thus, independent of the previous heat settings applied to the fibers, the plasticization effect due to benzoic acid exposition in different concentrations at fixed time seems to impose on these fibers a similar behavior, or the level of plasticization seems to be the same. It is clear also that the as-spun fiber with a less stable and more open structure presented lower values of *T_g* than did the drawn fiber. The higher disorientation of its amorphous region (as discussed in the first part of this article) promotes a more accessible way for the benzoic acid penetration, resulting in higher levels of chain flexibility.

The results obtained from DMTA (Figs. 3–9) show clearly the dislocation of the peak where *E''* is maximum (*T_g*) to lower temperatures as the concentration of benzoic acid increases. Also, it is pos-

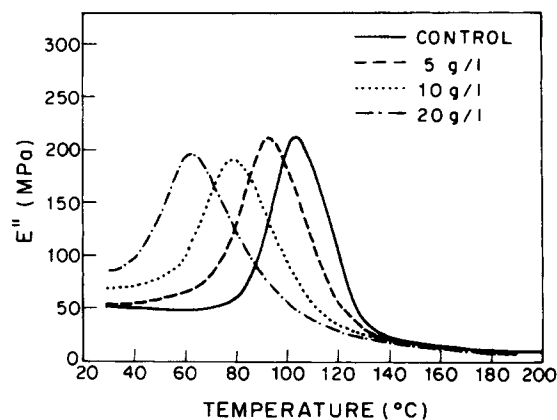


Figure 3 Loss modulus *E''* versus temperature for the as-spun fiber (preheat treatment T1) treated at different concentrations of benzoic acid (5, 10, and 20 g/L) and at a fixed time of half an hour.

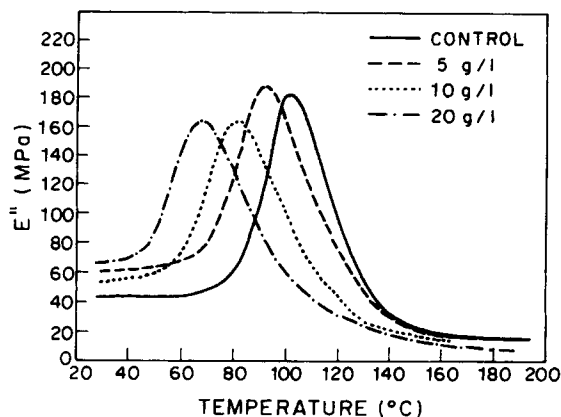


Figure 4 Loss modulus E'' versus temperature for the as-spun fiber (preheat treatment T3) treated at different concentrations of benzoic acid (5, 10, and 20 g/L) and at a fixed time of half an hour.

sible to observe the appearance of another transition peak in the range of temperatures of 130– to 160°C for the drawn fibers (2.8×) with the increase of benzoic acid concentration for a fixed time (Figs. 7–9). As can be seen the intensity of this peak increases similarly. This transition has been defined as the α_c transition and is related to the molecular movements within the crystalline phase,²¹ i.e., due to the viscous friction between crystallites or molecules inside the crystals. The time of exposition to the benzoic acid for a certain concentration does not seem to affect the intensity of the peak. The changes observed in the dynamic loss modulus curves versus temperature are not related to an isolated factor, but to a conjunction of factors such as chain flexibility, reorganization of the crystalline, and amorphous regions. Also, after treatment in benzoic acid, a shoulder is

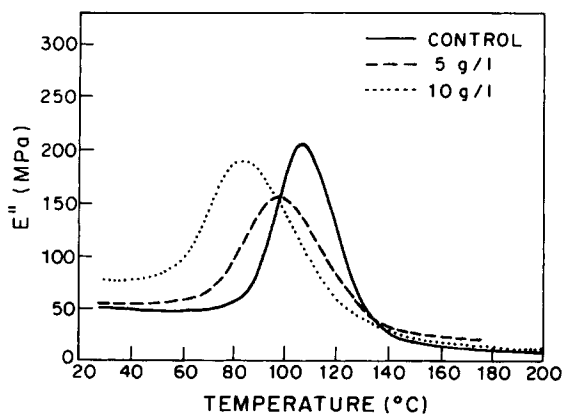


Figure 5 Loss modulus E'' versus temperature for the as-spun fiber (preheat treatment T1) treated at different concentrations of benzoic acid (5 and 10 g/L) and at a fixed time of 24 h.

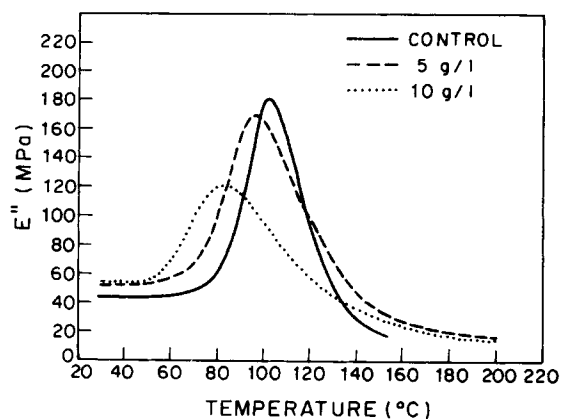


Figure 6 Loss modulus E'' versus temperature for the as-spun fiber (preheat treatment T3) treated at different concentrations of benzoic acid (5 and 10 g/L) and at a fixed time of 24 h.

observed at a temperature of 50°C, prior to the major α -dispersion peak (T_g) for all of the preheat-setted drawn fibers (2.8×). The appearance of this shoulder has been associated by Simal and Bell² with the presence of residual amounts of the benzoic acid used as a carrier. Simal and Bell² have demonstrated that subsequent boiling water treatment for 1 h can easily remove this shoulder, returning the α -dispersion weak to its original position. Thus, subsequent boiling water treatment showed effectiveness in the benzoic acid removal.

Another interesting observation related to these figures is the absence of this shoulder and the α_c peak in dynamic loss modulus curves for the undrawn fibers. However, when the analyses are directed toward the damping peak ($\tan \delta$) versus tem-

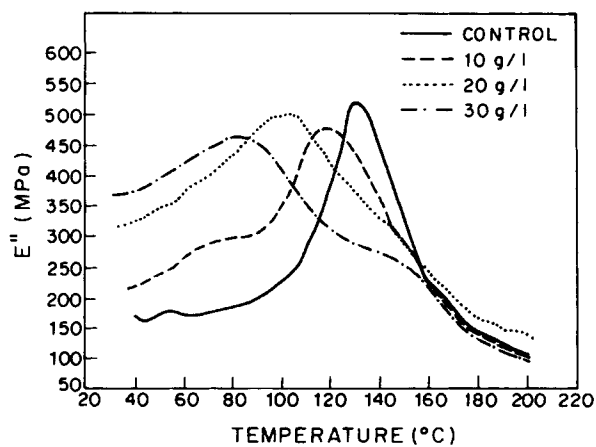


Figure 7 Loss modulus E'' versus temperature for the 2.8× fiber (preheat treatment T1) treated at different concentrations of benzoic acid (10, 20, and 30 g/L) and at a fixed time of half an hour.

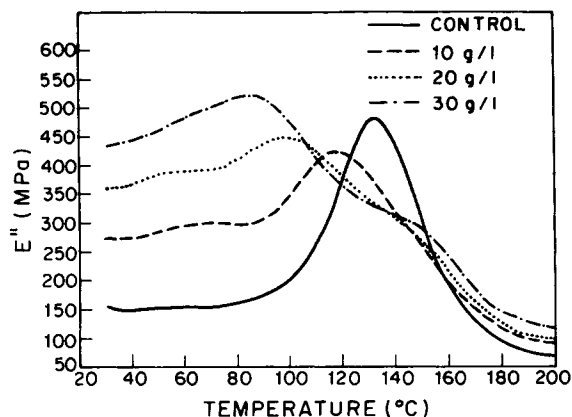


Figure 8 Loss modulus E'' versus temperature for the 2.8 \times fiber (preheat treatment T3) treated at different concentrations of benzoic acid (10, 20, and 30 g/L) and at a fixed time of half an hour.

perature (Figs. 10 and 11), an extension of the width of this peak is observed. Figure 11 shows a plateau-like peak, especially after treatment in benzoic acid at high concentrations and long times of exposition for the 2.8 \times fiber preheat treated for 8 h at boiling water temperature. Therefore, the enlargement of the $\tan \delta$ peak in the temperature range where the α_c relaxations are invisible (Figs. 7–9) might also be indicative of the presence of this transition in the as-spun fiber.

The DSC Analysis

In order to promote a better understanding of such behaviors, these samples were submitted to DSC analysis. The results of DSC analysis are shown in Figures 12–16.

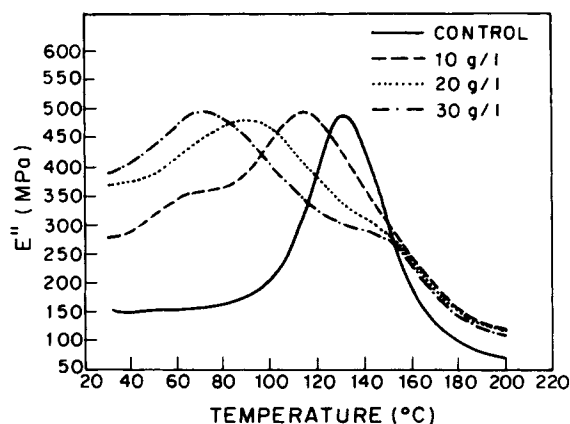


Figure 9 Loss modulus E'' versus temperature for the 2.8 \times fiber (preheat treatment T3) treated at different concentrations of benzoic acid (10, 20, and 30 g/L) and at a fixed time of 24 h.

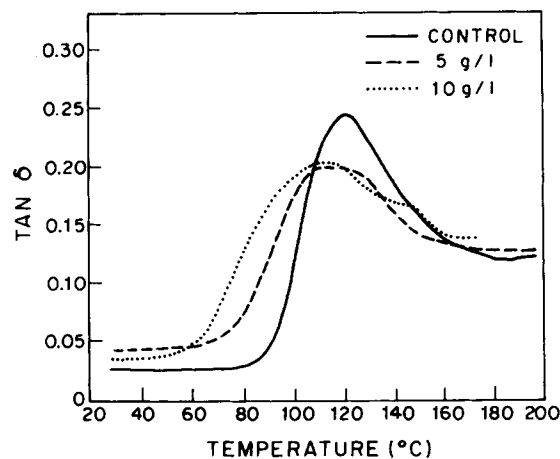


Figure 10 $\tan \delta$ versus temperature for the 0 \times fiber (preheat treatment T1) treated at different concentrations of benzoic acid (5 and 10 g/L) and at a fixed time of 24 h.

The thermograms show that under some conditions the first premelting peak (pm1) found in the DSC curves of the heat-setted fibers (treatments T1 and T3), as discussed earlier, remains after the benzoic acid treatments. Also, these thermograms reveal the appearance of a new premelting peak, which will be denoted here as pm2.

The crystallinities calculated from the area under these peaks are shown in Tables III and IV. In these tables, $\%C_1$, $\%C_2$, and $\%C$ represent the partial crystallinities calculated from the areas under the peaks pm1 and pm2 and under the main melting peak, respectively. The $\%C_T$ represents the global crystallinity or $\%C_T = (\%C_1 + \%C_2 + \%C)$.

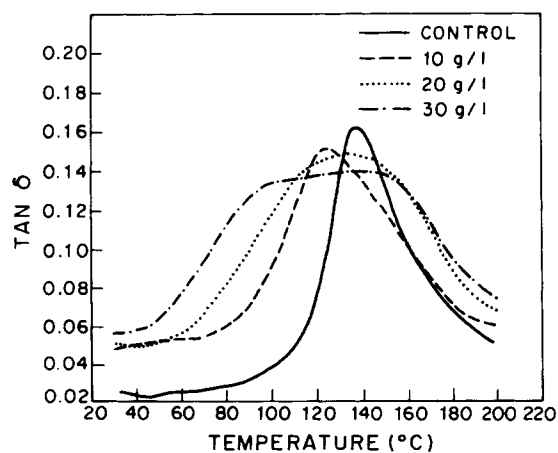


Figure 11 $\tan \delta$ versus temperature for the 2.8 \times fiber (preheat treatment T1) treated at different concentrations of benzoic acid (10, 20, and 30 g/L) and at a fixed time of 24 h.

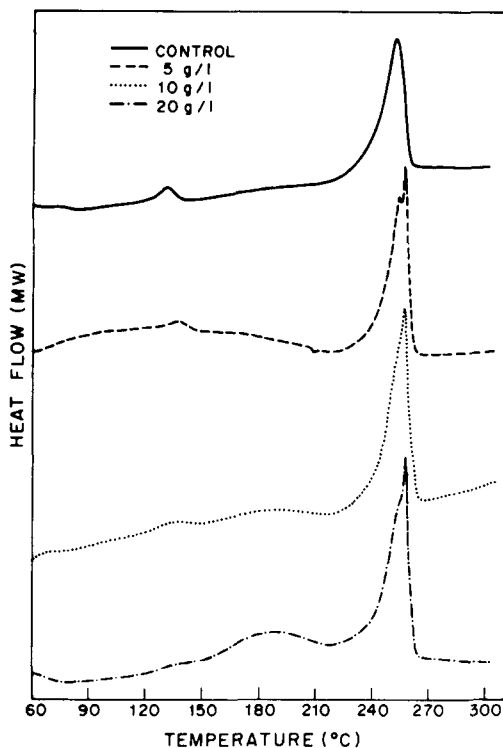


Figure 12 DSC thermograms of the as-spun fiber (pre-heat treatment T1) treated at different concentrations of benzoic acid (5, 10, and 20 g/L) at a fixed time of 48 h.

It is possible to observe in Figures 12–16 that the second premelting peak (pm2) occurs in a wider range of temperatures than the first premelting peak (pm1). This behavior seems to indicate the formation of a wider distribution of new crystals, as already⁶ discussed in the first part of this work. Analyzing the thermograms and the indicated tables, it is clear that the pm1 peak tends to disappear as the concentration and time of benzoic acid treatment increase.

Also, for the same experimental conditions, the appearance of the pm2 peak is accompanied by an increase of its area (increase of %C₂). It seems that a dislocation of the pm1 peak is occurring toward higher temperatures or that the pm1 peak has been transformed in a new pm2 peak. Similar results have been observed by Weigmann and colleagues³ for PET fibers treated with DMF. These effects are much more evident for the drawn fibers (2.8×). Someone may say that this phenomenon might be associated with the melting of the residual benzoic acid that remains inside the fibers during the DSC runnings. However, the melting temperatures of the benzoic acid is around 122°C, while the second premelting peak appears around 180°C. Therefore, this hypothesis can be discarded. Others could affirm that

the preheat settings (treatments T1 and T3) applied to the fibers were not enough to stabilize their structures, i.e., the fibers could present morphology changes after long times (more than 8 h) of exposition in boiling water, including the hydrolysis effect mentioned earlier.⁹

In order to verify such a hypothesis, the fibers previously heat setted (after treatments T1 and T3) were submitted to a new treatment in the presence of distilled boiling water for the same periods of time utilized in the benzoic acid treatments (up to 48 h). The results are given in Table V and Figure 17 (a and b).

The formation of the second premelting peak for both fibers was not verified, but a reasonable increase of the area under the first premelting peak (pm1) for the as-spun fiber only (Table V) was detected. Also, the crystallinities calculated from the main melting peak (%C) did not present any increase after long times of exposition in pure boiling water. These results indicate that the second premelting peak can be positively attributable to the benzoic acid action only. Thus, the benzoic acid action is promoting morphological changes in the preheat-setted fibers with the consequent elimination of the

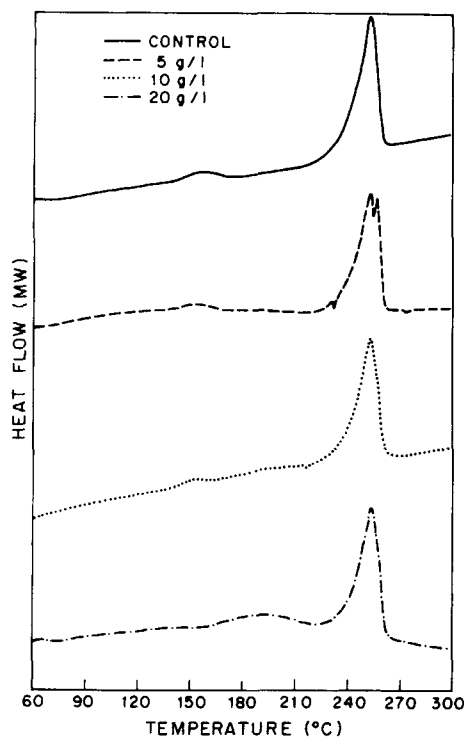


Figure 13 DSC thermograms of the as-spun fiber (pre-heat treatment T3) treated at different concentrations of benzoic acid (5, 10, and 20 g/L) at a fixed time of half an hour.

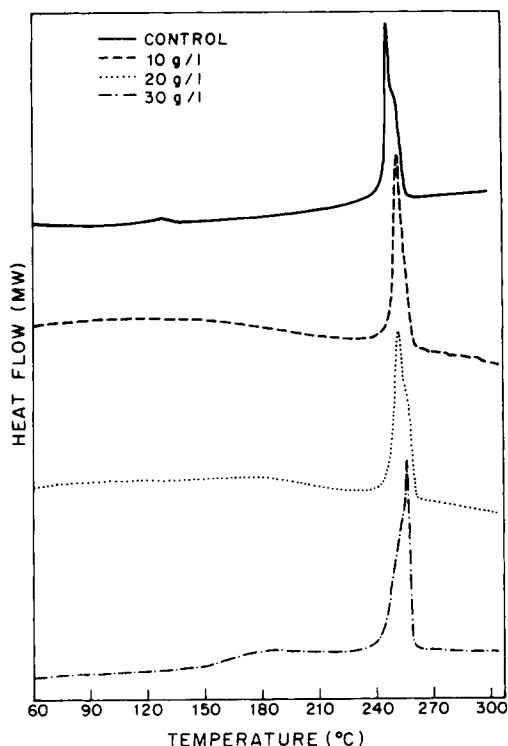


Figure 14 DSC thermograms of the 2.8 \times fiber (preheat treatment T1) treated at different concentrations of benzoic acid (10, 20, and 30 g/L) at a fixed time of 48 h.

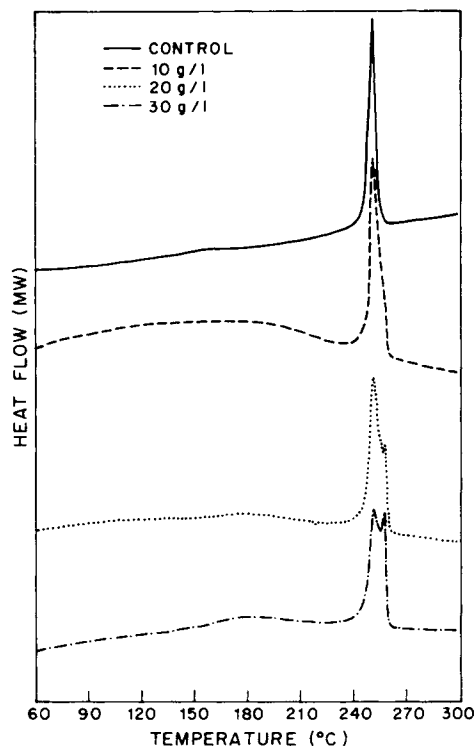


Figure 15 DSC thermograms of the 2.8 \times fiber (preheat treatment T3) treated at different concentrations of benzoic acid (10, 20, and 30 g/L) at a fixed time of 48 h.

morphological changes due to the water action only, i.e., the premelting peak (pm1) relative to small and more imperfect crystals is being transformed in the premelting peak (pm2) which is relative to more perfect crystals.

The morphological changes due to the water action are occurring much more easily for the undrawn fiber, which structure is originally more unstable. These effects, due to the water action, were not detected for the drawn fiber, confirming therefore that the applied preheat settings were enough to confer structural stability to this fiber. If the loss of molecular weight by hydrolysis of the ester groups is occurring due to the long⁹ times of exposition in pure boiling water, it seems that this possible effect is not supplanting or even interfering in the morphology changes of the analyzed fibers. The effect of the water treatment in the morphology changes of the fibers predominates over any loss of molecular weight due to hydrolysis. The increase of crystallinity (due to the increase of the area under the pm1 peak) may be fixing the structure and avoiding any substantial loss of molecular weight.

In contrast to the behavior mentioned previously (long times of treatment in pure boiling water) the partial crystallinity calculated from the main melt-

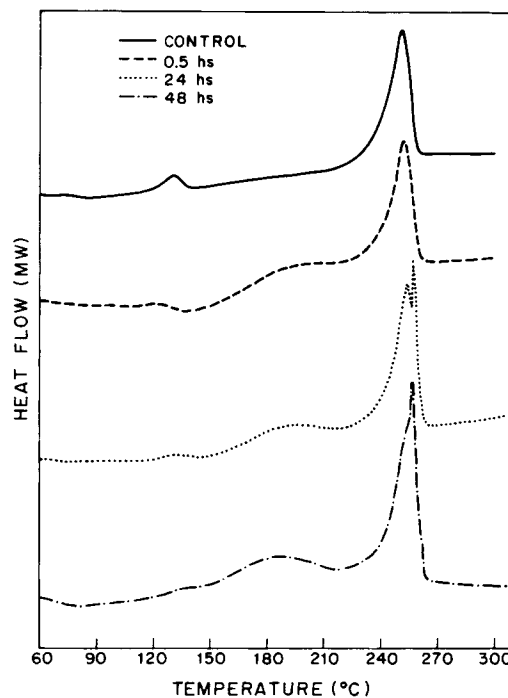


Figure 16 DSC thermograms of the spun fiber (preheat treatment T1) treated at different times (0.5, 24, and 48 h) at a fixed concentration of benzoic acid (20 g/L).

Table III Premelting Temperatures (pm_1 and pm_2), Main Melting Temperature (T_m), Partial Crystallinities ($\%C_1$, $\%C_2$, $\%C_3$), and Global Crystallinity ($\%C_T$) of the As-Spun Fiber

Heat Treatment	C (g/L)	t (h)	pm_1 (°C)	pm_2 (°C)	T_m (°C)	$\%C_1$	$\%C_2$	$\%C_3$	$\%C_T$		
T1	0	0.0	132	—	253	3	—	39	42		
		5	128	—	253	2	—	35	37		
		24.0	132	185	258	3	4	41	48		
		48.0	136	175	258	2	2	45	49		
	10	0.5	124	188	254	2	4	36	42		
		24.0	122	180	255	3	4	44	51		
		48.0	137	183	258	2	5	47	54		
		20	0.5	121	188	254	3	10	36	49	
	T3	0	24.0	131	188	259	1	10	47	53	
			48.0	—	184	258	—	15	48	63	
			5	0.0	155	—	253	—	3	37	40
			0.5	154	—	253	2	—	37	39	
10		24.0	132	157	255	1	1	42	44		
		48.0	132	—	258	2	—	44	46		
		0.5	152	194	253	1	5	37	43		
		24.0	130	183	259	1	5	43	49		
20	48.0	137	186	258	2	7	49	58			
	0.5	—	189	254	—	8	37	45			
	24.0	—	180	258	—	11	43	54			
	48.0	—	172	259	—	22	49	71			

Table IV Premelting Temperatures (pm_1 and pm_2), Main Melting Temperature (T_m), Partial Crystallinities ($\%C_1$, $\%C_2$, $\%C_3$), and Global Crystallinity ($\%C_T$) of the 2.8x Fiber

Heat Treatment	C (g/L)	t (h)	pm_1 (°C)	pm_2 (°C)	T_m (°C)	$\%C_1$	$\%C_2$	$\%C_3$	$\%C_T$		
T1	0	0.0	129	—	249	2	—	49	51		
		10	97	169	250	1	8	45	54		
		24.0	130	171	252	2	4	49	54		
		48.0	—	150	253	—	3	50	60		
	20	0.5	117	179	251	2	8	47	57		
		24.0	—	176	253	—	10	51	61		
		48.0	—	179	253	—	7	53	60		
		30	0.5	—	176	250	—	15	46	61	
	T3	0	24.0	—	180	252	—	11	50	61	
			48.0	—	184	257	—	12	55	67	
			10	0.0	158	—	252	2	—	47	49
			0.5	153	—	252	5	—	46	51	
20		24.0	150	—	252	6	—	47	53		
		48.0	—	196	253	—	7	52	59		
		0.5	—	180	250	—	3	47	50		
		24.0	—	177	253	—	4	49	53		
30	48.0	—	180	252	—	7	53	60			
	0.5	—	176	251	—	7	44	51			
	24.0	—	180	253	—	7	49	56			
	48.0	—	176	258	—	12	52	64			

Table V Premelting (pm_1) and Main Melting Temperatures and Respective Crystallinities ($\%C_1$ and $\%C$) of the As-Spun and 2.8x Fibers, Heat Treated at Different Times in Boiling Water Temperature

Fibers	Preheat Treatment	t (h)	pm_1 (°C)	T_m (°C)	$\%C_1$	$\%C$	$\%C_T$	
0x	T1	0	132	253	3	39	42	
		16	134	257	9	35	44	
		24	136	254	10	39	48	
		48	135	254	13	39	52	
	T3	0	155	253	3	37	40	
		16	152	253	13	35	48	
		24	158	254	15	37	52	
		48	157	254	13	36	50	
	2.8x	T1	0	129	249	2	49	51
			16	134	250	2	50	52
			24	135	251	2	48	49
			48	137	251	2	50	52
T3		0	158	252	2	47	49	
		16	141	251	3	47	50	
		24	141	251	4	48	52	
		48	140	251	3	48	51	

ing peak area ($\%C$) (Tables III and IV) is increasing with the concentration and time of treatment in the presence of benzoic acid. Consequently, the benzoic acid action is not only forming new crystals (related to the premelting peak pm_2) but also is altering the original crystalline region formed during the preheat settings (treatments T1 and T3), i.e., relative to the first premelting peak (pm_1) and the main melting peak, respectively.

Correlation Between DMTA and DSC Results

Comparing the range of temperatures, where the second premelting peak (pm_2) is occurring in the DSC thermograms (around 180°C) with the range of temperature where the α_c transition is occurring in the DMTA (from 140 to 160°C), it is possible to verify that the melting phenomenon is occurring in a subsequent range of temperature of the α_c relaxation. Therefore, both phenomena might be related to each other, i.e., the α_c transition corresponds to the relaxations of the new crystallites formed due to the benzoic acid action and the second premelting peak corresponds to the fusion of such crystals.

The absence of the α_c transition in the figures of loss modulus versus temperature (Figs. 3–6) for the as-spun fiber is difficult to explain, since it presented the second premelting peak in DSC analysis. However, considering the differences of orientation between the studied fibers (as spun and drawn 2.8×), it is possible that the DMTA is detecting such dif-

ferences. Probably, the more restrictive mobility of the chains due to the original orientation of the 2.8× fiber might define more easily the relaxations due to α_c transitions. As mentioned earlier, the enlargement of the damping peak in the range of temperature that would be related to such α_c relaxation (Fig. 10) is evident. As observed by the drawn fiber, such enlargement is occurring in the same way, forming a plateau-like peak when this fiber is exposed to high concentrations and for long times in benzoic acid solution (Fig. 11). Therefore, it seems that the absence of orientation makes the visualization of the α_c relaxation in the curves of loss modulus versus temperature difficult, but it can be detected in curves of $\tan \delta$ versus temperature through the enlargement of its peak (the enlarged peak surrounds the α and α_c relaxations). These differences of behavior due to the absence and presence of orientation in the fibers, seem to have a relationship with the theoretical concept of the loss modulus (E'') and the internal friction ($\tan \delta = \frac{E''}{E'}$). Therefore, the theo-

retical distinction between these concepts can help us to better understand the associated structural behavior of the fibers. The maximum heat dissipation per unit deformation occurs at the temperature where E'' is maximum. At low frequencies, this temperature is very close to the T_g of the sample, as determined by volume-temperature measurements.²¹ The loss modulus E'' is less prominent and goes

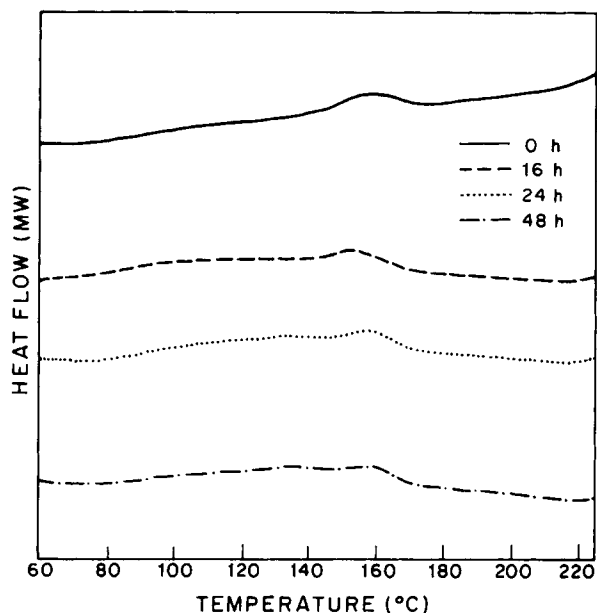
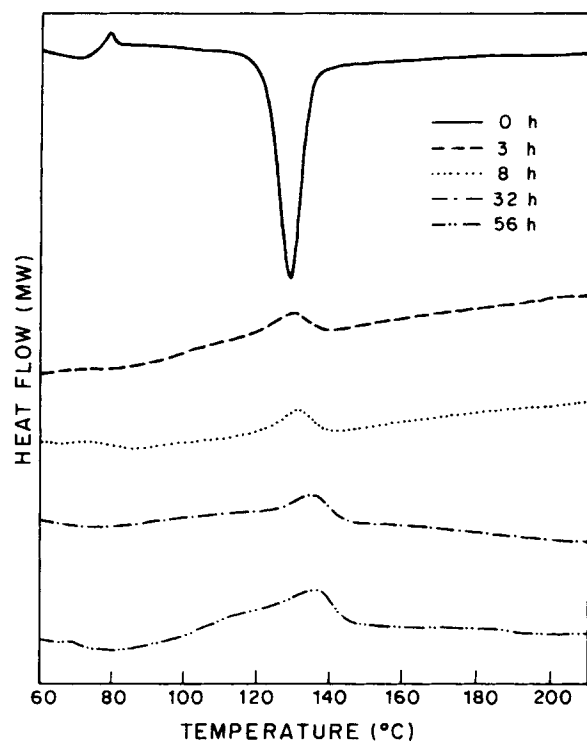


Figure 17 DSC thermograms of the preheat-setted as-spun fiber, heat treated at different times in boiling water: (a) preheat treatment T1; (b) preheat treatment T3.

through a peak at a slightly lower temperature (5–10°C) than does the damping peak ($\tan \delta$), or internal friction $\frac{E''}{E'}$. The damping peak is associated

with the partial loosening of the polymer structure, so that groups and small chain segments can move.²² Therefore, the $\tan \delta$ generally responds in a systematic way to the volume fraction of any given relaxing phase, whereas the other loss parameter does not.²³ Thus, the absence of orientation in the as-spun fiber facilitates the cooperative motion of the chain segments, making a clear distinction between the relaxing transitions (α and α_c) when the loss modulus (E'') is the analyzed parameter difficult.

CONCLUSIONS

The changes on the structural parameters analyzed by x-ray and FTIR analysis as well as the changes on the DSC thermograms were helpful to show a comprehensive understanding of the morphology of the PET fibers after the different heat treatments were applied. The differences in orientation (undrawn and 2.8 \times) between the studied fibers promoted a different behavior concerning the amount of trans conformer being generated due to the applied heat treatments. The dry heat treatment of 7 h at 130°C is more effective in increasing the trans conformer content for the 2.8 \times fiber than the as-spun one, with a subsequent increase in the intermolecular packing. When this fiber is submitted to a subsequent 1 h boiling water treatment, a decrease in the trans conformer is observed, while for the as-spun fiber, the opposite is observed for the same conditions of heat treatments. Therefore, it seems that the water treatment is affecting the chain packing of the amorphous region for the 2.8 \times fiber, while in the case of the undrawn fiber, the increase of trans conformer content might be related to an increase of crystalline perfection.

From the DSC analysis, the existence of a pre-melting peak for both fibers was observed, which would reflect the type of morphology developed in these fibers after the applied heat treatments. Also, the DSC analysis reflected the presence of a wider distribution of smaller crystals for the undrawn fiber than for the 2.8 \times fiber.

A subsequent exposition of these fibers to benzoic acid treatments at different concentration and times showed its effectiveness to plasticize these fibers. The plasticization of the as-spun fiber occurred in the first half-hour exposition in the benzoic acid solution, while the plasticization effect for the 2.8 \times fiber occurred at up to 24 h of treatment. This behavior reflected once more the structural stabiliza-

tion difference between these fibers, in decorrence of their orientation differences.

Also the DSC analysis of these benzoic acid-treated fibers revealed that the first premelting peak that appeared after the heat-setting treatments of the fibers, is dislocating toward higher temperatures (appearing as a second premelting peak). Therefore this second premelting peak has been related to the morphological changes due to benzoic acid action only, and the first premelting peak (pm1), relative to small and more imperfect crystals, is being transformed in the second premelting peak, which is relative to more perfect ones.

The DMTA results show a α_c relaxation peak for the benzoic acid-treated samples with increased intensity as the benzoic acid concentration increases. Since the second premelting temperature is occurring at temperatures around 180°C and the α_c relaxation is occurring in the range of temperature from 140 to 160°C, it is possible to conclude that the α_c transition corresponds to the relaxation of the new crystallites formed after benzoic acid treatment and the second premelting peak corresponds to the fusion of such crystals.

Finally, the plasticization effect due to benzoic acid exposition at different concentrations and times is generating a more complex structure in the PET fibers. It is acting by breaking the intermolecular bonds, relaxing the residual orientations, and decreasing T_g , which will induce higher chain flexibility.

This effect continuing for long times will promote an increase of the global crystallinity by chain folding and the generation of new and more perfect crystallites inside the amorphous regions, in addition to the preexisting crystals, which are responsible for the main melting peaks in DSC analysis. This complex structure should contain also the presence of voids, as described in earlier work by Simal and Bell² and in the first section of this paper.

ACKNOWLEDGMENT

We express our gratitude to FAPESP and CAPES (Brazil), which were responsible for the financial part of this work. Also, we are thankful to Leine Aparecida Silva for her typewriting work.

REFERENCES

1. R. H. Peters, *Textile Chemistry, Vol. III, The Physical Chemistry of Dyeing*, Elsevier Scientific Publ. Co., New York, 1975.
2. A. L. Simal and J. P. Bell, *J. Appl. Polym. Sci.*, **30**, 1195 (1985).
3. H. D. Weigmann, M. G. Scott, and A. S. Ribnick, *Textile Res. J.*, **47**, 761 (1977).
4. H. D. Weigmann, M. G. Scott, and A. S. Ribnick, *Textile Res. J.*, **48**, 4 (1978).
5. H. J. Oswald, E. A. Turi, P. J. Harget, and Y. P. Khanna, *J. Macromol. Phys.*, **B13**(2), 231 (1977).
6. M. V. S. Rao, R. Kumar, and N. E. Dwelt, *J. Appl. Polym. Sci.*, 4439 (1986).
7. J. Gacén, F. Bernald, and J. Maillo, *Textile Chemistry Col.*, 31 (1988).
8. A. L. Simal and J. P. Bell, *J. Appl. Polym. Sci.*, **30**, 1679 (1985).
9. B. H. Knox et al., *Textile Res. J.*, **51**, 549 (1981).
10. G. Groeninckx, H. Reynaers, H. Berghmans, and G. Smets, *J. Poly. Sci. Phys. Ed.*, **18**, 1311 (1980).
11. H. M. Cullerton, M. S. Ellison, and J. R. Aspland, *Textile Res. J.*, **50**, 594 (1990).
12. L. E. Alexander, *X-Ray Diffraction Methods in Polymer Science*, Wiley Interscience, New York, 1969.
13. D. R. Subramanian and A. Venkataraman, *J. Macromol. Sci.*, **B18**(2), 177 (1980).
14. N. V. Bhat and S. G. Naik, *Textile Res. J.*, **54**(12), 868 (1984).
15. H. M. Heuvel and R. Huisman, in *Integration of Fundamental Polymer Science and Technology*, L. A. Kleintjens and P. J. Lemstra, Eds., 536, Elsevier Appl. Sci. Publ., London, 1986.
16. Shaow-Burn Lin and Jack Koenig, *J. Poly. Sci. Poly. Phys. Ed.*, **21**, 2067 (1983).
17. H. W. Siesler, in *FTIR Characterization of Polymers*, Hsuo Ishida, Ed., Vol. 36, Plenum Press, New York, 1987.
18. A. K. Jain and V. B. Gupta, *J. Appl. Polym. Sci.*, **41**, 2931 (1990).
19. G. W. Urbanczyk, *J. Appl. Sci.*, **38**, 55 (1989).
20. H. M. Heuvel and R. Huisman, *J. Appl. Polym. Sci.*, **30**, 3069 (1985).
21. T. Murayama, *Dynamic Mechanical Analysis of Polymeric Materials*, Elsevier Scientific Publ. Co., New York, 1978.
22. L. E. Nielsen, *Mechanical Properties of Polymers and Composites*, Vol. 1 and 2, Marcel Dekker, Inc., New York, 1974.
23. R. E. Wetton, in *Developments in Polymer Characterisation—Chapter 5*, J. V. Dawkins, Ed., Elsevier Applied Science Publishers, London, 1986.

Received December 19, 1995

Accepted January 5, 1996